*Eur. J. Mech. B/Fluids*, **17**, n° 4, 549–560, 1998

# Experimental evidence for a new type of stretched vortex

**P. PETITJEANS [a]*, J. H. ROBRES [a], J. E. WESFREID [a], N. KEVLAHAN [b]**

ABSTRACT. – Experimental measurements performed under conditions which reproduce most of the dynamical characteristics of the natural evolution of vorticity filaments in turbulent flows are presented here. Strong deviations from the Burgers vortex (which is a non-confined stretched vortex model) are observed and analyzed. © Elsevier, Paris

## 1. Introduction

Recent recognition of the role of small scale filaments and layered vortex sheets in turbulence have led to interest in the dynamical behavior of vortex structures with concentrated vorticity. Indeed, the instability, reconnection, merging and breakdown of these vortical structures are at the origin of intermittence in turbulent energy dissipation. Numerical simulations (Siggia, 1981; Jimenez, 1991) and experiments (Cadot *et al.*, 1995) show clearly that the dynamics of stretched filaments are responsible for the deviation from the Gaussian behavior observed in turbulence statistics. Many open questions remain about these dynamics, especially concerning the vortex breakdown processes and the existence of finite time singularities.

Structures with concentrated vorticity arise in many different situations. For instance, concentrated vorticity can appear as a result of instabilities such as the Bénard-Von Karman vortex street, and in shear flows. If the vorticity field is stretched, especially in the case of structures resulting from instabilities, the vorticity may be strongly enhanced. This process occurs naturally in the complex field of a turbulent flow. In these flows, vorticity can be locally stretched by the local velocity gradients. Indeed, most of the time the stretching in such flows is applied locally (and not globally). This is the reason a Burgers model (where the stretching is constant and uniform) may not be the relevant model for these structures. Some other models have already been proposed such as the cusp model (Farge and Holschneider, 1991), or a model based on fractal analogy (Vassilicos and Brasseur, 1996).

In order to better understand the detailed mechanisms of the evolution of a stretched vortex, we have performed a new experiment where isolated stretched vortices are produced. These vortices are observed and their characteristics are determined quantitatively. The goal of our experiment is to impose a physical stretching on the vorticity of a stable boundary layer developed on flat plates. The applied stretching amplifies the initial vorticity by a factor of order one hundred in the experiment described in this paper. This evolution is observed by means of flow visualization (Laser Induced Fluorescence), and velocity measurements (Laser Doppler Anemometry). Most of the dynamical characteristics of the evolution of vorticity filaments in turbulent flows are reproduced in our channel, in a well-controlled experimental situation.

[a] Laboratoire de Physique et Mécanique des Milieux Hétérogènes, UMR CNRS 7636, École Supérieure de Physique et de Chimie Industrielles, 10, rue Vauquelin, 75005 Paris, France

[b] Laboratoire de Météorologie Dynamique, École Normale Supérieure, 24, rue Lhomond, 75005 Paris, France

* Correspondence and reprints


0997-7546/98/04/© Elsevier, Paris

In this paper we will present experimental velocity measurements of a non uniform stretched vortex.

## 2. Experiment

### 2.1. Experimental set-up

The experiments are performed in a water channel, where the flow is generated by gravity from a constant level tank. The channel itself, of order 2 m length is made of plexiglas. It consists of two sections: the first section generates a laminar flow and the second is the working section. The water enters the first section of the channel through small holes directed perpendicularly to the main flow in order to avoid jet effects. The next section is a 2D divergent channel of rectangular cross section. It is 60 cm long and the divergent angle is less than 6°. Next is a channel 20 cm long filled with straws aligned in the direction of the flow, followed by a 2D convergent section which reduces the cross section to a rectangular section of 12 cm wide by 7 cm high. The purpose of this first part of the channel is to produce a well-controlled laminar flow. The second part of the channel consists of a straight section 60 cm long. In the middle of this section, a slot is made in each lateral side which is used to create a controlled suction of the main flow. At the end of this section, the flow leaves through a system whic allows accurate measurement of the flowrate. In the first half of this straight section (before the suction), the laminar flow creates a boundary layer on each side of the channel. Since the suction slots are located on the lateral walls, only the vorticity coming from the boundary layers on the upper and lower walls is stretched by the suction. This stretching is parallel to the initial vorticity. The flowrates of the suctions on each sides are identical, and can be controlled and measured. If the suction is constant at all slots, vortices are generated in phase on the upper wall and on the lower wall, and their vorticity is of opposite sign (Petitjeans *et al.*, 1997a). Depending on the suction rate and on the flow rate of the main flow, these vortices interact, merge, or remain separate from each other or from the next pair of vortices generated on the same wall.

In the experiments described in this paper, the suction is generated by a hole of 0.6 cm diameter on each lateral side located 0.5 cm up from the bottom of the channel (*Fig.* 1). The initial vorticity, stretched by these suctions, is enhanced and produces a vortex on the lower wall only. Below a certain flow rate at the exit of the channel, the vortex remains stationary at this location (Petitjeans *et al.*, 1997b), sometimes with a low-amplitude precession. Above this flowrate, the vortex is elongated in the direction of the flow and may break up, in which case another one is generated in its place, and so on.

In addition, in the experiments reported here a step of 1.1 cm high shown in Figure 1 was placed just before the suction. This step produces a more stable vortex with a smaller precessional motion. Let us recall that stretched vortices can be generated even in the absence of this step. In fact, the step was built to force the vortex to form in its side where a half-ellipse was cut out. The idea was to impose an elliptic form on the vortex in order to study the instabilities of an elliptic stretched vortex. However, the vortex does not form at that place, but rather a little bit higher, and is even more stable than without this step, which actually increases the roll-up effect!

In the following, $x$ is the axis in the streamwise direction, $y$ is the vertical axis directed from the bottom to the top, and $z$ is the spanwise axis parallel to the initial vorticity. $(0,0,0)$ is the origin at the bottom of the channel, in the stretching axis, and in the center with respect to the spanwise direction. The velocity components are $(U,V,W)$, or $(U_r,U_\theta,U_s)$ with respect to the center of the vortex.

The velocity field can be measured with a one component laser Doppler anemometry system (LDA). The probe of the LDA is moved by a 3D displacement system. Vortices are also visualized by injection of fluorescent dye and argon laser light (laser induced fluorescence). The dye (fluoresceine) is injected as a sheet through a slot in the bottom of the channel, 2 cm upstream from the suction (*Fig.* 1). A cross-section of the visualization at the middle of the channel is shown Figure 2. From these visualizations, it is possible to measure the components

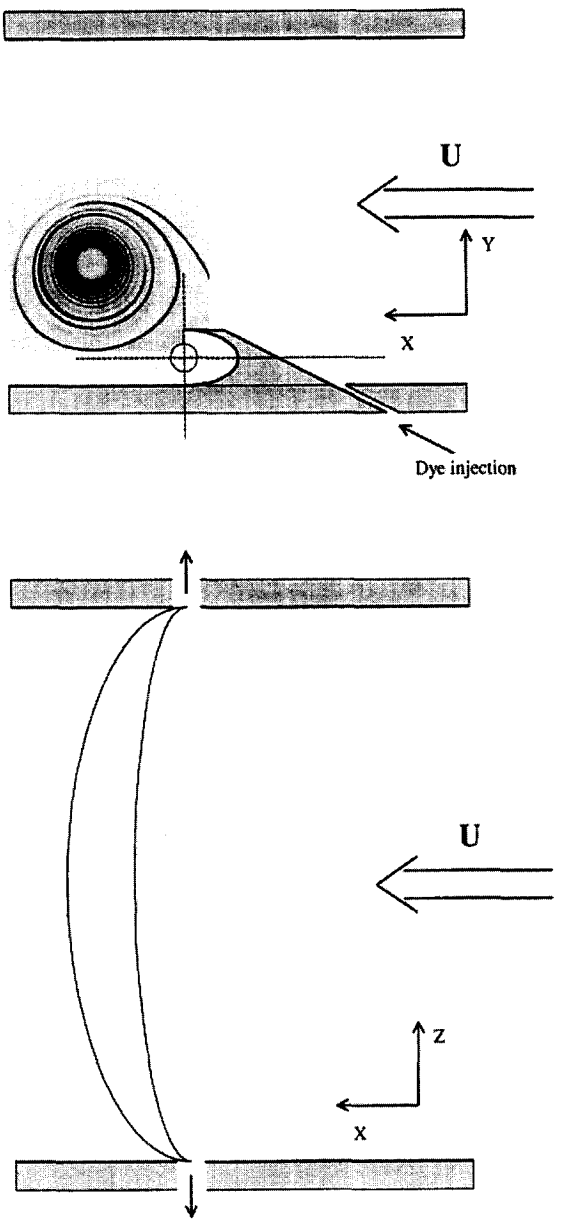


Fig. 1. – Section of the experimental set-up where stretched vortices are produced. Because of the flow and its own rotation, the vortex takes the form of a "banana".

$U_r(r)$ and $U_\theta(r)$ of the vortex, by following the front of the dye in time, taking a frame each 0.04 s (our video records 25 images/s). The front of the "streaklayer", which gives the trajectory of a given fluid particle, does in fact follow the streamlines. Indeed, the flow is only weakly non-stationary because of the slow precession of the vortex (Hama, 1962). Each image gives the position $(x, y)$ of the front of the dye, and $(x_0, y_0)$ of the location of the center of the vortex. The spatial resolution is 0.05 mm. From these values, the coordinates $(r, \theta)$ of the front of the dye can be deduced at each time step, as well as the velocity component $U_r(r)$ and $U_\theta(r)$. The radial velocity $U_r(r)$ is obtained by taking the derivative of the fit of the curve $r(t)$, the angular

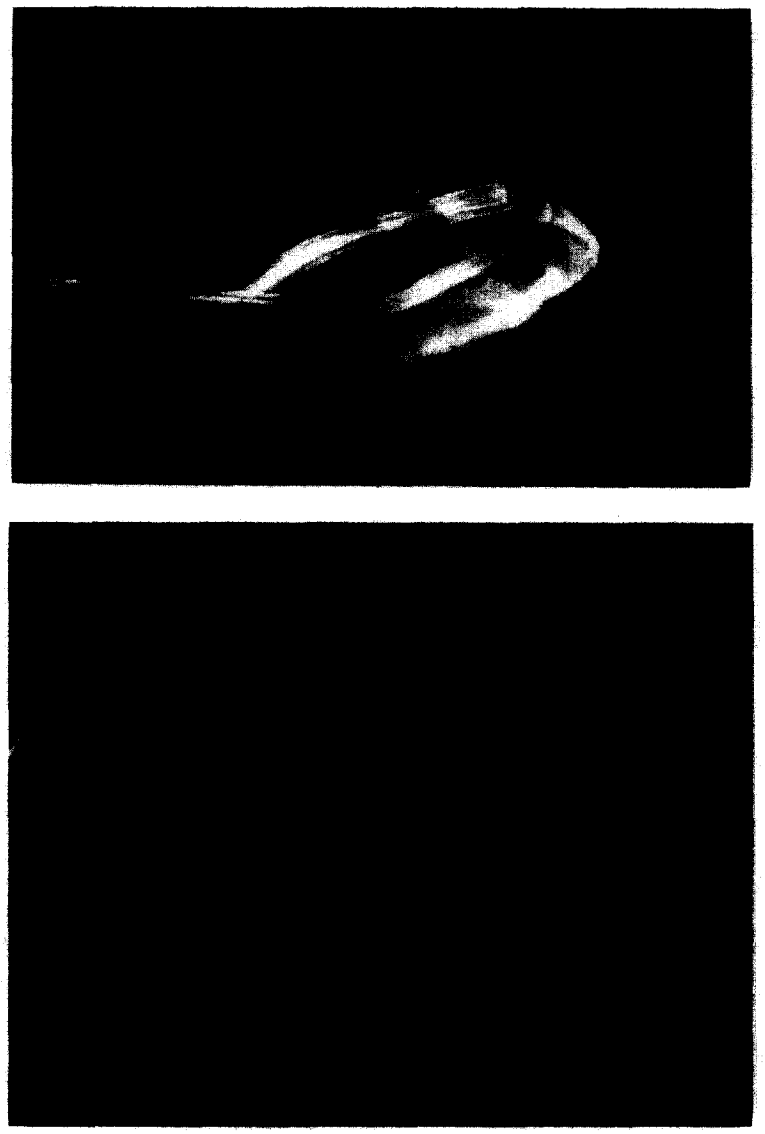

Fig. 2. – The first picture shows the whole view of a stretched vortex. The flow comes from the right-bottom towards the left-top. The second photo shows a cross-section of a vortex. The vertical size of the picture is about 2 cm.

velocity $\Omega(r)$ is obtained from the derivative of the fit of the curve $\theta(t)$, and the azimuthal velocity $U_\theta(r)$ is obtained from $U_\theta(r) = r \cdot \Omega(r)$.

### 2.2. Results

In the experiments described below, the flow rate at the exit of the channel is zero, while the flow rate of the suction is 3.2, 4.0, 5.0, or 6.0 l/mn for each side. In these cases the vortex is stable and almost stationary (there is only a small precession which will be described later).

An example of the streamwise velocity profiles just before the step ($x$ = –2 cm) is given in Figures 3a, 3b in case of a stretching flowrate of 3.2 l/mn. $U(z)_{y=3.5\text{ cm}}$ shows a boundary layer profile deformed by an acceleration on the sides due to the suction 2 cm upstream. $U(y)_{z=0}$ shows the boundary layer profile with a small recirculation at the bottom just before the step. The streamwise velocity profile in the vertical direction at

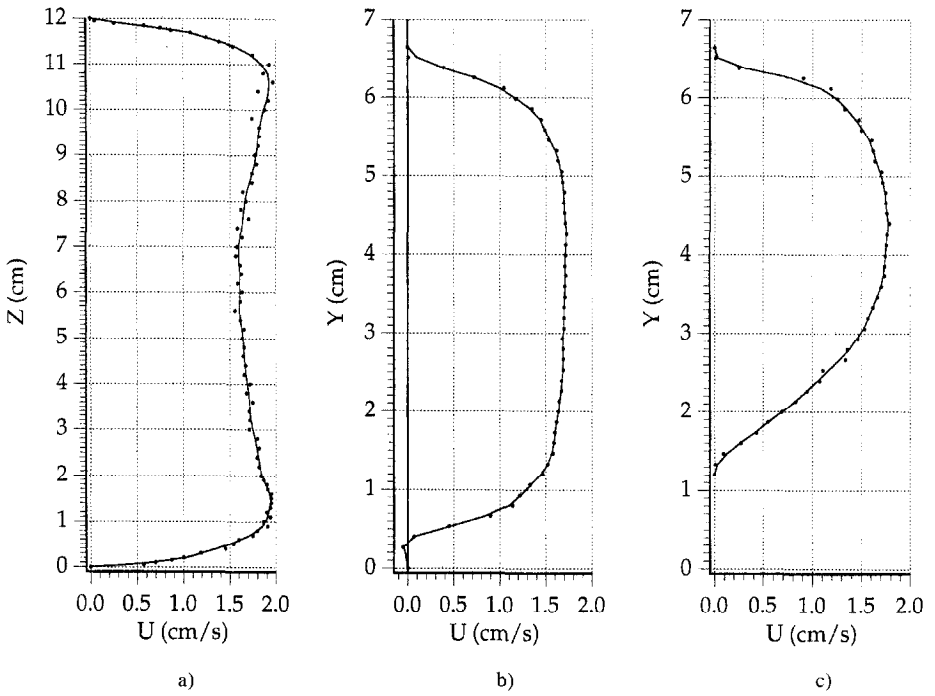


Fig. 3. – (a) Streamwise velocity profile $U$ along the spanwise axis $z$ for $y = 3.5$ cm (*i.e.* the center of the channel in the vertical direction). The flow is faster near the walls because of the suction 2 cm downstream. (b) Vertical streamwise velocity profile.
These two graphs show the streamwise velocity profiles before the step. (c) The third graph shows the same profile just at the end of the step. This graph gives the initial vorticity which will be enhanced by the stretching just after this section. This initial vorticity is of order 0.9 $s^{-1}$.

the end of the step $U(y)_{z=0}$ is shown Figure 3c. This profile gives the initial vorticity which will be stretched by the suction. From this figure, the initial vorticity can be estimated to be of order $\omega_1 \sim 0.9\, s^{-1}$.

The vortex created by the stretching of the initial vorticity takes the form of a "banana" sketched in Figure 1. The center of the vortex precesses slowly with an amplitude of order 1 mm. Figure 4 gives an example of the motion of the center of the vortex during 32 s, obtained by following the center in a video tape of the visualization. The vortex precesses in the same direction as its rotation, as observed in other experiments (Pinton, 1997; Andreotti, 1997; Piva, 1998). Figure 5 shows the distance $r$ between the front of the dye and the center of the vortex as a function of the angle of rotation for four different stretchings. We were able to determine the position of the front of the dye until a radius $r$ as small as 0.2 cm. Below this value, the front of the dye could no longer be distinguished any more. At the beginning of the rolling up process, the distance $r$ does not follow a monotonic law as a function of the angle as long as the dye layer has not reached the vortex itself (before, the vortex is not circular due to the proximity of the wall and the step). After three or four turns around the vortex, the curve tends to a logarithmic law defining a logarithmic spiral motion $r \sim \exp(-\alpha\theta)$ where $\alpha$ is a constant (Vassilicos and Brasseur, 1996). In order to give more information about the structure of the spiral, the distance between two layers of dye $\Delta r = r(\theta_i) - r(\theta_i + 2\pi)$ is given as a function of the number of turns $\Delta r(n)$ (*Fig.* 6). For instance, this can be used to determine if a self-similar pattern arises or not. Figure 7 confirms the logarithmic spiral motion, in showing the evolution of $\partial\theta/\partial r$ as a function of $r$. Indeed, a logarithmic spiral $r \sim \exp(-\alpha\theta)$ yields $\partial\theta/\partial r \sim 1/r$, as is observed in this figure (at least for a stretching flowrate $Q < 6$ l/mn). Note that a logarithmic spiral has a Kolmogorov dimension $D_K = 1$, *i.e.* it has a trivial self-similar structure. Only an algebraic spiral ($r \sim \theta^\alpha$) has a non-trivial self-similar structure and a Kolmogorov dimension $D_K > 1$.

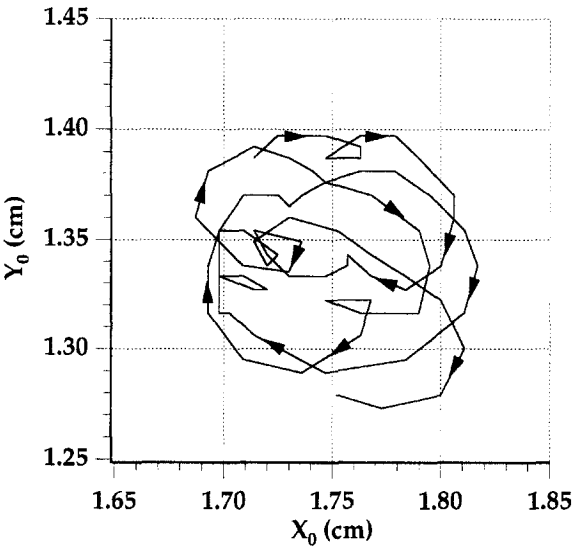


Fig. 4. – Variation of the position of the center of the vortex with time during 32 s, for a stretching flow-rate of 3.2 l/mn. The precession turns in the same direction as the vortex with an amplitude of order 1 mm.

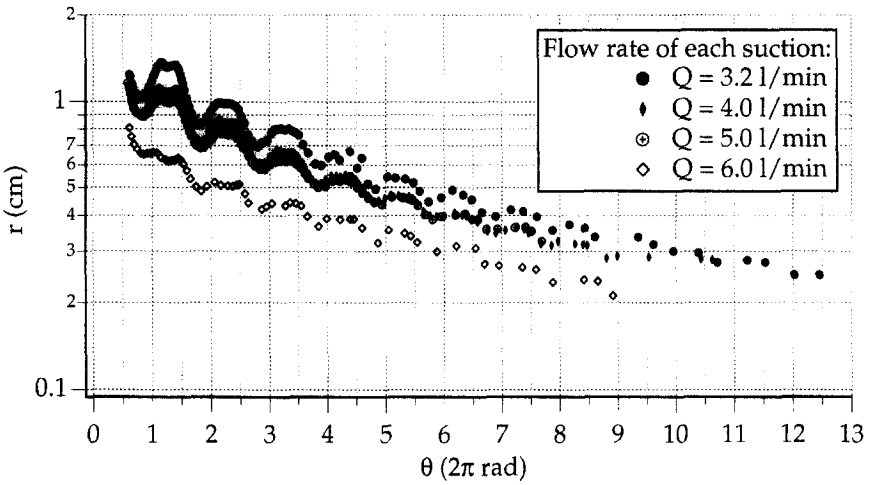


Fig. 5. – The front of the dye sheet is followed in time (every image step, *i.e.* every 0.04 s). The distance of the front from the center of the vortex gives the radius $r$ of the vortex as a function of the angle $\theta$, for four different stretching flow rates. The curves tend to a logarithmic law defining a logarithmic spiral motion $r \sim \exp(\alpha\theta)$.

As explained before, knowing $r(t)$ and $\theta(t)$ allows us to deduce the radial velocity $U_r(r)$ by taking the derivative of the fit of the curve $r(t)$ (*Fig.* 8), the angular velocity $\Omega(r)$ (*Fig.* 9) can be found by the derivative of the fit of the curve $\theta(r)$, and the azimuthal velocity $U_\theta(r) = r\Omega(r)$ (*Fig.* 10a). Figure 10b shows the profile $U_\theta(r)$ under the same conditions measured by laser Doppler velocimetry.

The stretching velocity $U_s(r, s)$ has also been measured by laser Doppler velocimetry. Figure 11 shows the radial dependence of the stretching velocity $U_s(r)_{s\,\text{fixed}}$ for two different spanwise position $z$ = 2.5 cm and $z$ = 4.5 cm from the center of the channel. We observe that the stretching essentially occurs in a small region around the vortex axis. Figure 12 shows the axial dependence of the stretching velocity $U_s(s)_{r=0}$ along the axis of the vortex (which is not straight, see the sketch in Figure 1). From the center of the channel (in the spanwise direction) to about half way from the side, the stretching, *i.e.* the gradient of the stretching velocity

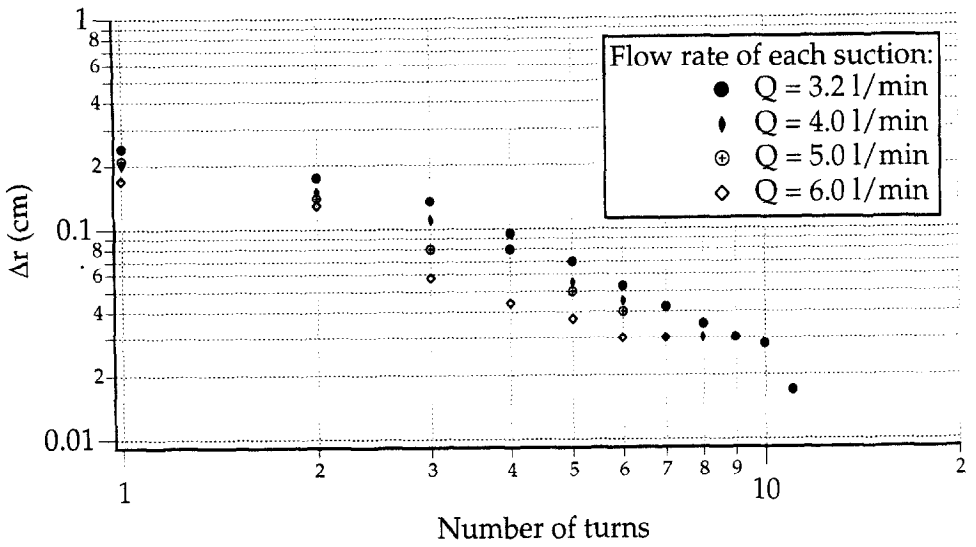


Fig. 6. – The distance between two layers of dye $\Delta r = r(\theta_i) - r(\theta_i + 2\pi)$ is given as a function of the number of turns $\Delta r(n)$.

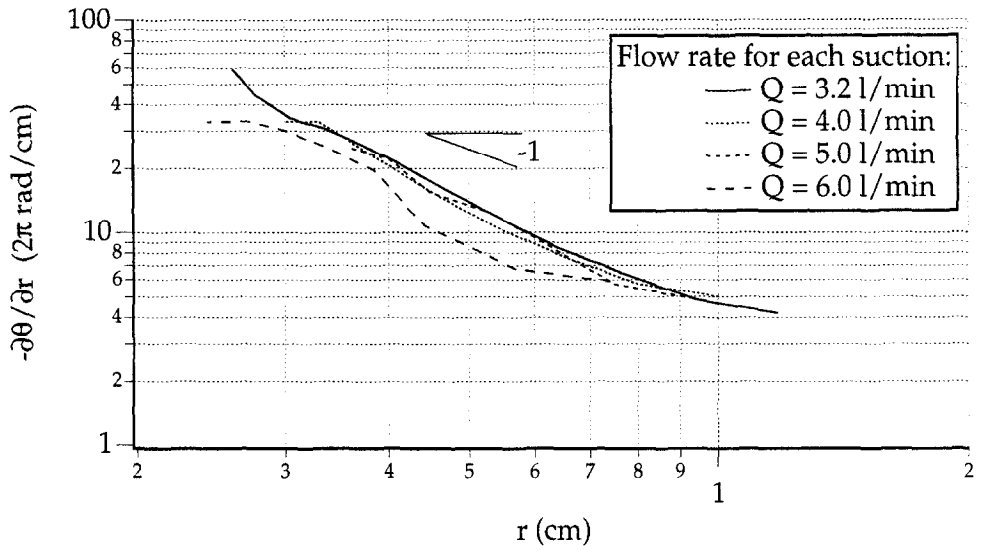


Fig. 7. – The evolution of $\partial\theta/\partial r$ is plotted as a function of the radius $r$, for four different stretching flow rates, and shows a scaling law $\partial\theta/\partial t \sim 1/r$, confirming the logarithmic spiral motion $r \sim \exp(-\alpha\theta)$.

along the vortex axis, is constant. In the second half, the stretching increases linearly (the stretching velocity follows roughly a quadratic law as a function of the curvilinear coordinate). The channel can be separated into two parts along the spanwise axis: the middle two-thirds where the stretching is constant, and the sides where the stretching increases linearly in the direction of the suction slots.

The measurements presented in Figure 11 illustrate the main point of our paper. Indeed, it is clear that the stretching is not transversally uniform (*i.e.* it does depend on the distance $r$ from the axis). Such a result was to be expected since in our experiment the suction is located at a particular position on the lateral walls. We claim that this is also the case for most naturally occurring stretched vortices, and is particularly the case for filaments of vorticity in turbulent flows, where local stretching strongly enhances the vorticity (parallel to the

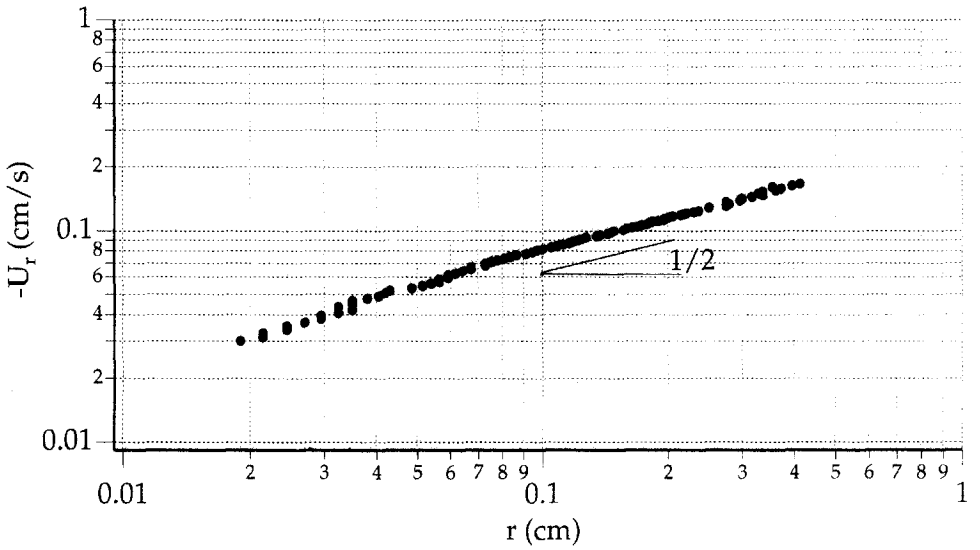


Fig. 8. – The radial velocity $U_r(r)$ is plotted as a function of the radius $r$ for a stretching flow-rate of 3.2 l/mn, and shows that $U_r(r) \sim r^{1/2}$.

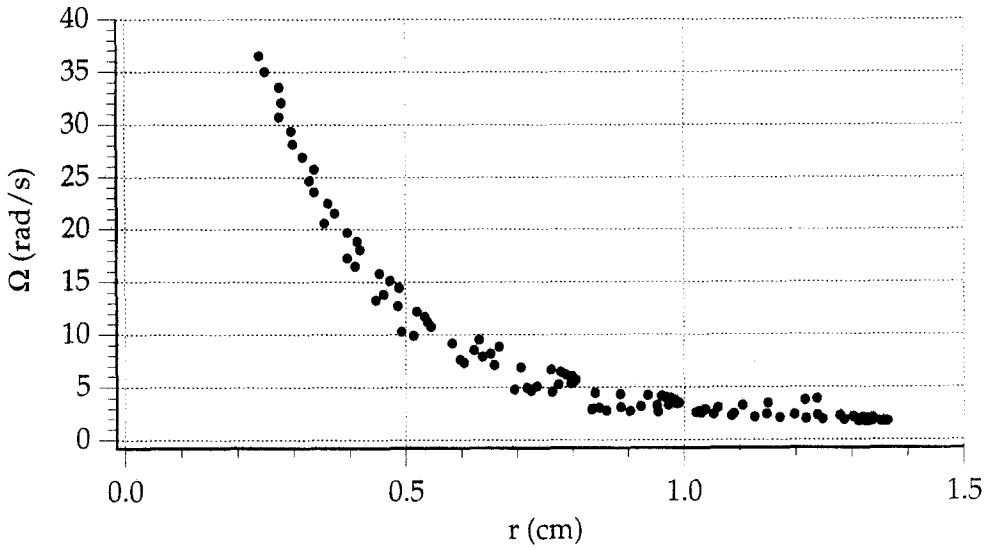


Fig. 9. – The angular velocity $\Omega(r)$ is plotted as a function of the radius $r$ for a stretching flow-rate of 3.2 l/mn.

stretching) of the turbulent flow. A model often used to describe these vortices is the Burgers vortex, which is the stationary vortex created by constant and uniform stretching (viscous diffusion of vorticity exactly balances vorticity amplification by stretching):

(1) $$U_z = Az$$

(2) $$U_r = -\frac{1}{2} Ar$$

(3) $$U_\theta = \frac{\Gamma}{2\pi r}\left\{1 - \exp\left(-\frac{A}{4\nu} r^2\right)\right\}$$

a)

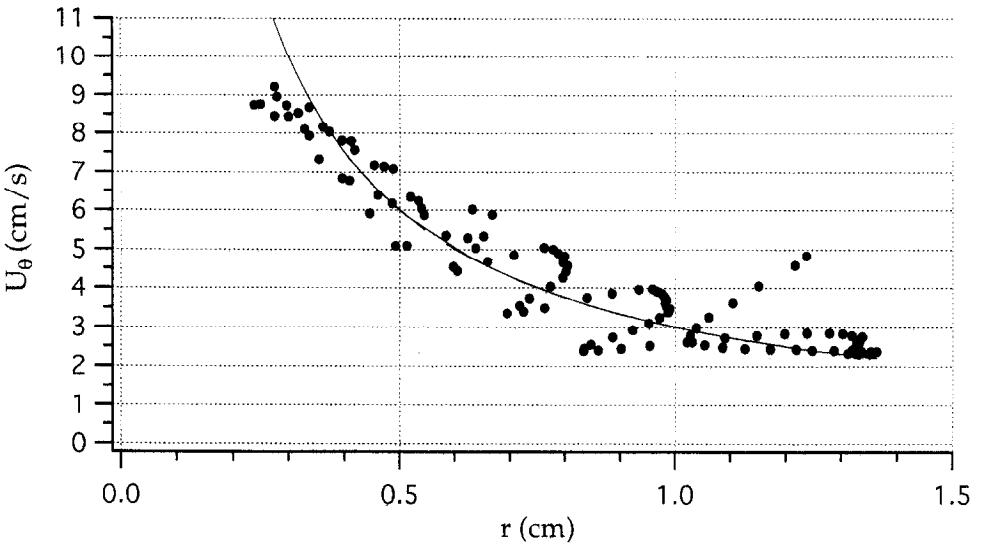


b)

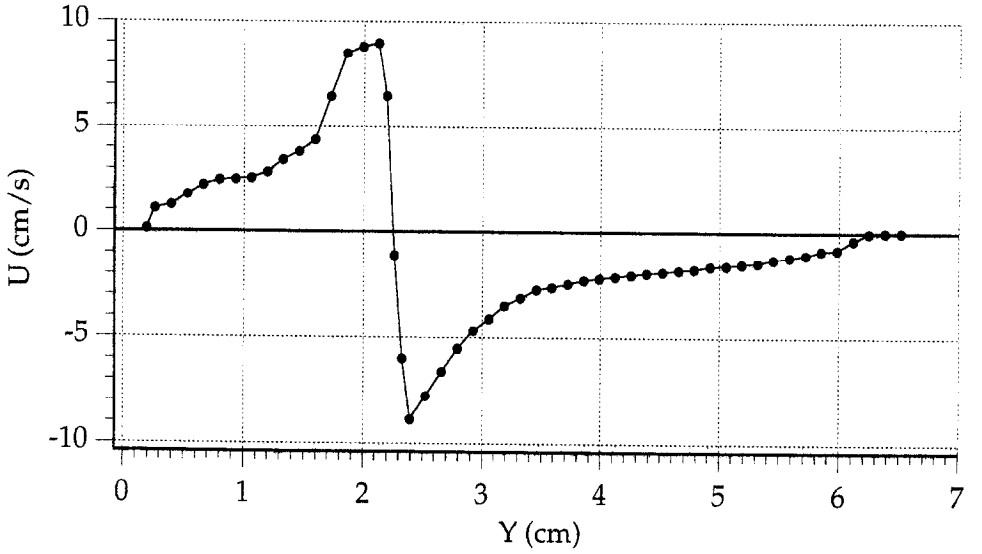


Fig. 10. – (a) The azimuthal velocity $U_\theta(r) = r\Omega(r)$ is plotted as a function of the radius $r$ for a stretching flow-rate of 3.2 l/mn. The line shows the fit $U_\theta = c/r$ outside the core of the vortex.
(b) The azimuthal velocity $U_\theta(y)$ measured with laser Doppler velocimetry for the same stretching is plotted as a function of the vertical coordinate $Y$.

$$\omega_z = \frac{\Gamma A}{2\pi} \exp\left(-\frac{A}{4\nu} r^2\right) \tag{4}$$

where the constant $A$ is the stretching rate, $\Gamma$ is the circulation, $\nu$ is the kinematic viscosity, and $\omega$ is the vorticity. This model cannot represent our kind of stretched vortex, which is not stretched uniformly.

Figure 8, which represents the radial velocity $U_r(r)$ shows that this velocity scales as $r^{1/2}$. From other measurements of $U_r(r)$, we observe that it does not depend on $z$, at least far enough from the walls (see later). From Figures 11 and 12, we observe that the stretching velocity $U_z(r, z)$ scales as $r^{-1/2}z$. The stretching

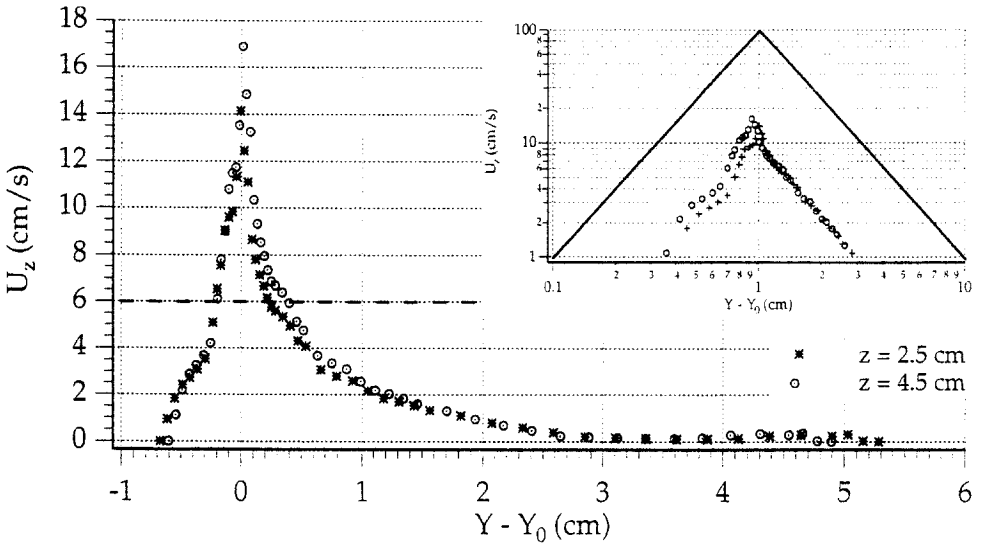


Fig. 11. – The stretching velocity $U_z$ is plotted as a function of the vertical coordinate $Y$ for two different spanwise positions $z$ for a stretching flow-rate of 3.2 l/mn. These velocity profiles, obtained with laser Doppler velocimetry, show that $U_z \sim r^{-1/2}$. A Burgers vortex would have given the dashed line.

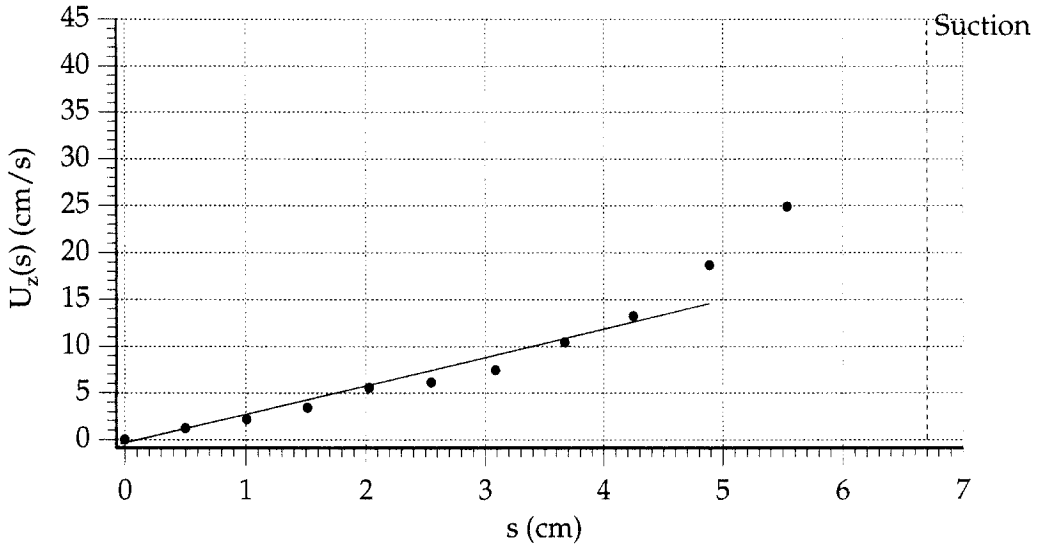


Fig. 12. – The stretching velocity $U_z$, for a stretching flow-rate of 3.2 l/mn, is plotted as a function of the curvilinear coordinate $s$ along the vortex core for one half of the channel. From the center of the channel ($z$ = 0 to about $z$ = 4 cm, the stretching is a linear function fof the curvilinear coordinate, giving then a constant stretching (gradient of the stretching velocity). In the second part, from $z$ = 4 cm to the wall where the suction is applied, the stretching velocity is more like a quadratic law of $s$, giving then a stretching which increases linearly with $s$.

velocity scales linearly with the curvilinear axis $s$ ($\sim z$ at these positions), at least far enough from the lateral walls, *i.e.* in about 3/4 of the width. These two measurements are independent ($U_r(r)$ is obtained by following the front of the dye in a visualization, and $U_z(r,z)$ is obtained with a laser Doppler velocimetry system) and satisfy the continuity equation. So, we obtain

$$U_r = -\frac{2}{3} A r^{1/2} \tag{5}$$

$$U_z = Azr^{-1/2} \tag{6}$$

where $A$ is a constant.

The important point is that the stretching here is confined around the axis of the vortex. (6) implies the existence of an azimuthal vorticity which one can prove has no feedback effect on the axial vorticity. (5) and (6) are now used to solve the axial-vorticity equation where we assume, at order zero, that the axial-vorticity is stationary. We obtain:

$$\omega_z = \omega_0 \exp\left(\frac{-4A}{9\nu} r^{3/2}\right) \tag{7}$$

Then, from Kelvin's circulation theorem, the azimuthal velocity is:

$$U_\theta = \frac{c}{r} \int_0^r x \cdot \exp\left(\frac{-4A}{9\nu} x^{3/2}\right) dx \tag{8}$$

where $c$ is a constant. The core of the vortex, corresponding roughly to the region between the two maxima of velocity $U_\theta(r)$, cannot be explored using the measurements based on visualization of the front of the dye. Therefore, it is not possible to check the validity of this expression (8) in the core. We can only check that the azimuthal velocity scales as $1/r$ outside the core, as expected far from the core of the vortex (*Fig.* 10a). The difference between our vortex and Burger's vortex (3) should be apparent only in the core region.

The expressions (5) to (8) are not an exact solution of the Navier-Stokes equations. Work is in progress in order to add the effects of the non-stationarity and the effects of the non-axial component of the vorticity. In addition, another experiment of controlled vortex stretching will be performed where there will be no walls and no mean flow to perturb the vortex.

## 3. Conclusion

Experimental observations show that most stretched vortices in nature in general and in turbulence in particular are non-uniformly stretched, which is inconsistent with the basic assumptions of the Burgers model. On the basis of our measurements, the expressions for the velocity field and vorticity field we have presented should be a good starting point in order to built a new model of a non transversly uniform stretched vortex.

**Acknowledgements.** – We would like to thank Alain Pumir for helpful discussions.

REFERENCES

ANDREOTTI B., 1997, private communication.

CADOT O., DOUADY S., COUDER Y., 1995, Characterization of the low-pressure filaments in a three-dimensional turbulent shear flow, *Phys. Fluids*, **7**, 630-646.

FARGE M., HOLSCHNEIDER M., 1991, Interpretation of two-dimensional turbulence energy spectrum in terms of quasi-singularity in some vortex core, *Europhys. Lett.*, **15**, 737-743.

HAMA F. R., 1962, Streaklines in a perturbed shear flow, *Phys. Fluids*, **5**, 644-650.

JIMENEZ J., 1991, On small scale vortices in turbulent flows, *Phys. Fluids*, **A-4**, 652-654.

PETITJEANS P., WESFREID J. E., ATTIACH J. C., 1997a, Vortex stretching in a laminar boundary layer flow, *Exp. Fluids*, **22**, 351-353.

PETITJEANS P., WESFREID J. E., 1997b, Vortex stretching and filaments, *Applied Scient. Research*, **57**, 279-290.

PINTON J. F., 1997, private communication.
PIVA M., 1998, private communication.
SIGGIA E. D., 1991, Numerical study of small-scale intermittency in three-dimensional turbulence, *J. Fluid Mech.*, **107**, 375-406.
VASSILICOS J. C., BRASSEUR J. G., 1996, Self-similar spiral flow structure in low Reynolds number isotropic and decaying turbulence, *Phys. Rev. E*, **54**, 467-485.

(Received 14 October 1997,
revised 27 February 1998,
accepted 31 March 1998)